Supporting information:

Docking screens for dual inhibitors of disparate drug targets for Parkinson's disease

Mariama Jaiteh[1,†], Alexey Zeifman[1,†], Marcus Saarinen[2], Per Svenningsson[2], Jose Bréa[3], Maria Isabel Loza[3], and Jens Carlsson[1,*]

[1] Science for Life Laboratory, Department of Cell and Molecular Biology, Uppsala University, BMC Box 596, SE-751 24 Uppsala, Sweden.

[2] Center of Molecular Medicine, Department of Physiology and Pharmacology, Karolinska Institute, Stockholm, Sweden.

[3] USEF Screening Platform-BioFarma Research Group, Centre for Research in Molecular Medicine and Chronic Diseases, University of Santiago de Compostela, 15706 Santiago de Compostela, Spain.

[†]Contributed equally to this work.

Table of contents

Supporting Figures **Page**

Supporting Tables

References

Supporting Figures

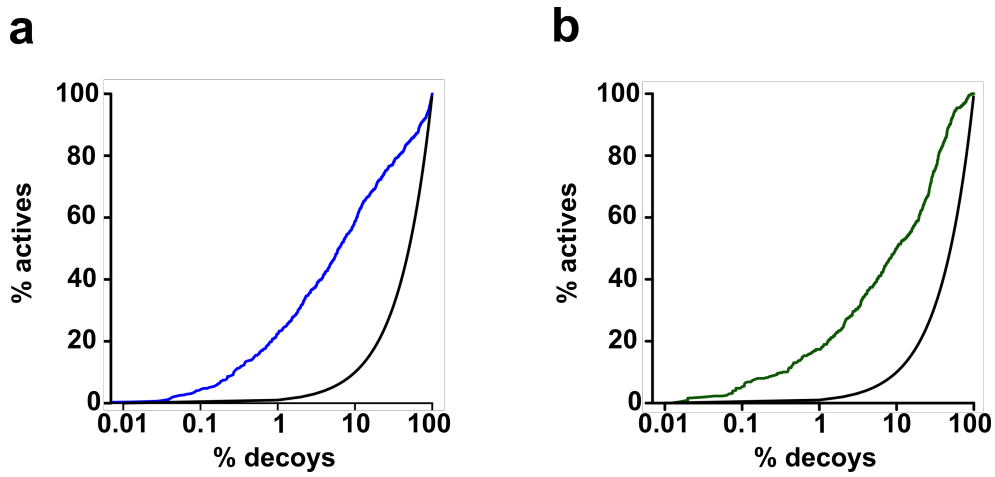

Figure S1. Enrichment curves for known A_{2A}AR and MAO-B ligands. Receiver operator characteristic (ROC) curves for databases of ligands and property-matched decoys ranked by molecular docking. The percentage of ligands and decoys identified in the ranked database are shown on the y- and x-axis, respectively. The solid black line represents random enrichment of ligands. (**a**) Enrichment of A_{2A}AR ligands and (**b**) MAO-B ligands by the crystal structures used in the virtual screen are shown.

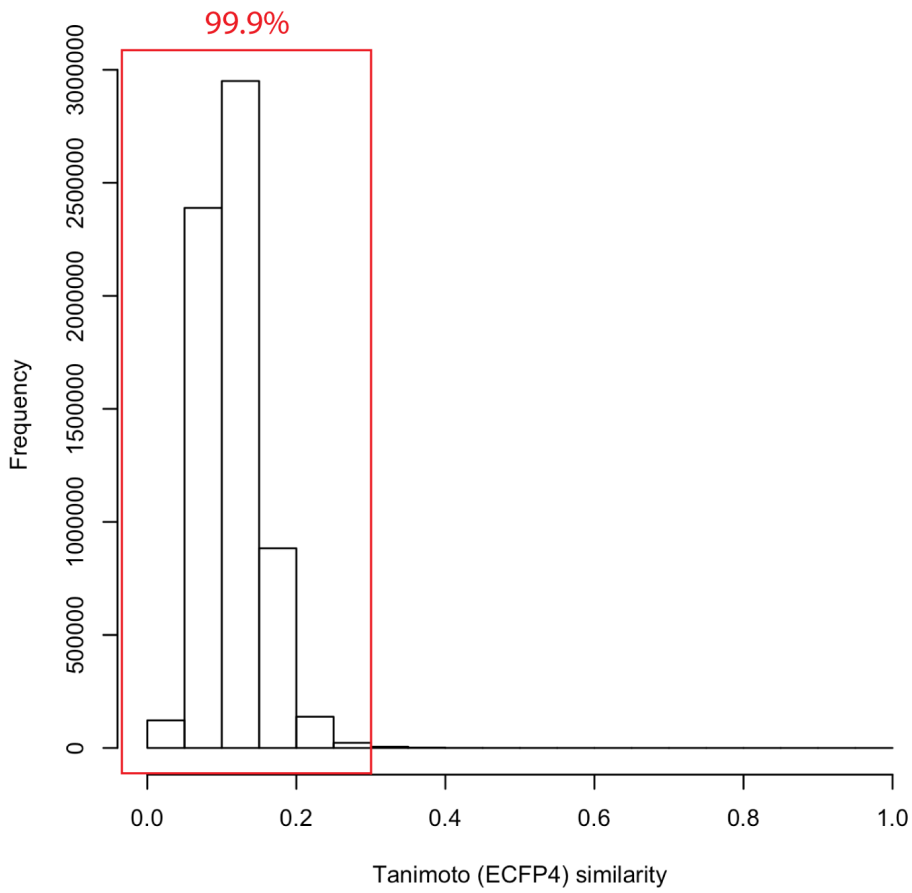

Figure S2. 2D similarity between known $A_{2A}AR$ and MAO-B ligands. The Tanimoto similarity (ECFP4 fingerprints) was calculated between all $A_{2A}AR$ (3898 compounds) and MAO-B (1671 compounds) ligands from the ChEMBL database[1].

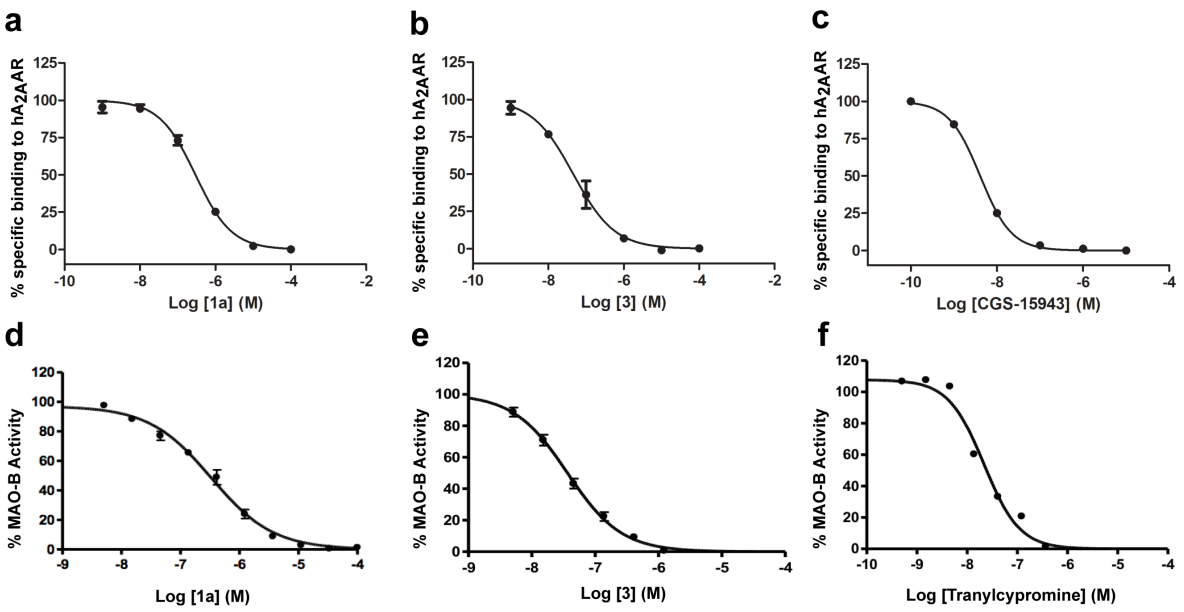

Figure S3. Dose-response curves for compounds 1a, 3, and controls. (**a-c**) Radioligand displacement curves for compounds **1a**, **3**, and control (CGS-15943, K_i = 1.3 nM, n=1) at the $A_{2A}AR$. K_i values for compounds **1a** and **3** (Table 2 and Table 1, respectively) were determined from three independent experiments and the error bars represent the SEM. (**d-f**) Inhibition of MAO-B by compounds **1a**, **3** and control (Tranylcypromine, IC_{50} = 22 nM, n=1). IC_{50} values for compounds **1a** (n = 3, Table 2) and **3** (n = 2, IC_{50} = 40 ± 10 nM obtained with modified MAO-B assay conditions compared to Table 1, see methods for details).

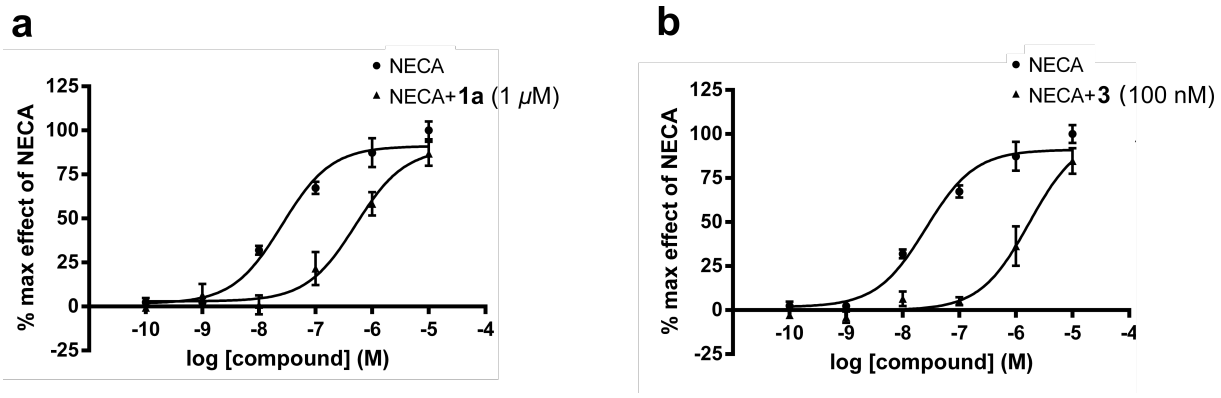

Figure S4. Functional assays for compounds 1a and 3 at the $A_{2A}AR$. Functional assay based on measuring the production of cAMP for the agonist NECA in the presence or absence of compounds (**a**) **1a** and (**b**) **3**. The NECA dose-response curve shows a right-shift in the presence of both compounds, as expected for competitive antagonism.

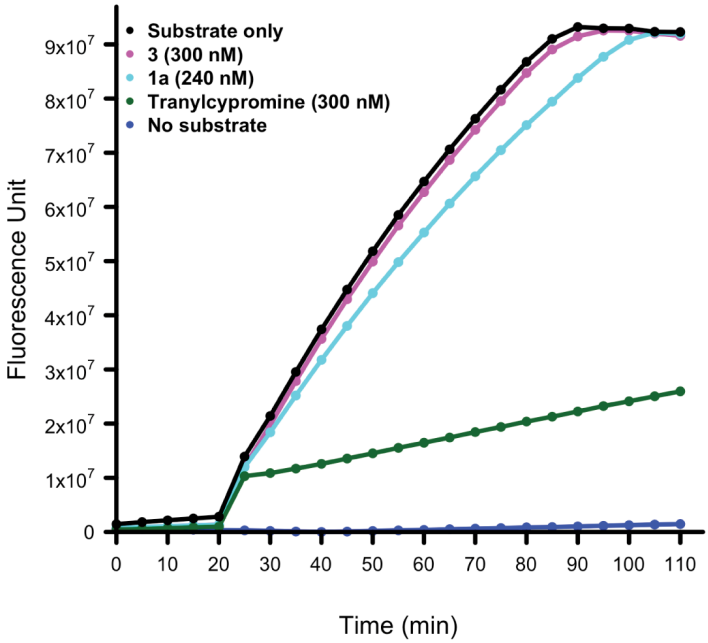

Figure S5. MAO-B reactivation assays for compounds 1a and 3. MAO-B was pre-incubated in presence of substrate and either compounds **1a**, **3**, or the irreversible inhibitor tranylcypromine. An excess of substrate was added after 20 minutes. The measured fluorescence increased for compounds **1a** and **3**, as expected for reversible inhibition, whereas only a small increase was observed for tranylcypromine that was used as control.

Supporting Tables

Table S1. Ligand enrichment by crystal structures of $A_{2A}AR$ and MAO-B. The selected structures are marked in green.

MAO-B crystal structure (chain)	Adjusted LogAUC[a]	$A_{2A}AR$ crystal structure	Adjusted LogAUC[a]
2V61 (B)	28.4	4EIY	25.7
2V5Z (B)	28.0	3PWH	25.1
2V5Z (A)	27.8	3EML	25.1
2V60 (A)	27.4	3UZC	23.1
2V60 (B)	27.4	3RFM	21.4
4A7A (B)	27.0	3VGA	21.1
3PO7 (A)	26.7	3UZA	18.5
3PO7 (B)	26.7	3REY	17.5
2V61 (A)	26.7	3VG9	13.6
2C70 (A)	26.4		
4A79 (A)	26.3		
4A7A (A)	26.2		
2C70 (B)	25.5		
4A79 (B)	25.0		
3ZYX (A)	17.1		
3ZYX (B)	16.0		

[a]Known ligands and property-matched decoys were docked to the crystal structures. The performance of each crystal structure was quantified using the adjusted LogAUC[2], which has values >0 if ligand enrichment is better than random.

Table S2. Comparison of the binding sites of $A_{2A}AR$ and MAO-B using the ProBiS webserver (http://probis.cmm.ki.si/).

		Target binding site[a]	
Query binding site		MAO-B	$A_{2A}AR$
	MAO-B	4.21	−1.83
	$A_{2A}AR$	−1.83	4.16

[a]Binding site was defined as all residues within 7 Å of the co-crystallized ligand.

Table S3. The 24 compounds selected from the molecular docking screens.

ID	Rank[a]	Smiles	ZINC code[b] (Screening Library)	Vendor
1	54	c1ccc(cc1)C(=O)Nc2[nH]c3ccccc3n2	C12729683 (F)	Enamine
2	386	c1ccc(cc1)COC(=O)c2c(nn(n2)c3ccccc3)N	C01424478 (L)	VitasM
3	50	COc1cccc(c1)COC(=O)c2c(nn(n2)c3ccccc3)N	C01429452 (L)	VitasM
4	470	C[C@H]1C(=O)Nc2cc(ccc2O1)Nc3c4c(c5ccccc5o4)ncn3	C32808492 (L)	Enamine
5	146	Cn1c2c(c(=O)[nH]c1=O)n3cc([nH]c3n2)c4ccc(cc4)Cl	C00506266 (L)	VitasM
6	243	Cc1ccc2c(c1)n3cnnc3c(n2)NCc4cccc(c4)OC	C04835077 (L)	ChemDiv
7	257	Cn1c2c(ccc(n2)C(=O)Nc3ccccc3F)c(=O)n(c1=O)C	C32796391 (L)	Enamine
8	278	c1ccc2c(c1)ccc(n2)C(=O)Nc3[nH]c4ccccc4n3	C05262984 (L)	Enamine
9	34	Cn1c(=O)[nH]c(=O)n2c1ncc2CC(=O)Nc3cccc4c3cccc4	C28527220 (L)	Princeton-Bio
10	464	c1ccn2cc(nc2c1)C(=O)Nc3nc4c(cc(cc4s3)F)F	C12525602 (L)	Enamine
11	72	c1ccc(cc1)c2cc([nH]n2)c3nc4c5ccccc5ncn4n3	C32815325 (L)	Enamine
12	482	CSc1ccc(cc1)CNc2c3nncn3c4ccccc4n2	C04910228 (L)	ChemDiv
13	1	c1ccc(cc1)Nc2nccc(n2)c3cccnc3	C29559018 (F)	VitasM
14	169	c1cc(cc(c1)F)c2[nH]nc(n2)c3cccnc3	C40164161(F)	InnovaPharm
15	181	Cc1cccc(n1)Nc2nc(cs2)C(=O)NC	C62162472 (F)	LifeChemicals
16	202	c1ccc2c(c1)ccc(n2)NCc3ccccn3	C21026386 (F)	Enamine
17	212	c1ccc2c(c1)c(=O)[nH]c(n2)/C=C/c3cccnc3	C08738871 (F)	VitasM
18	215	c1ccc2c(c1)[nH]c(n2)c3[nH]c4ccccc4n3	C00097949 (F)	VitasM
19	256	c1ccc(cc1)c2cc(=O)c(n[nH]2)c3ccccc3	C08672859 (F)	Specs
20	271	Cc1ccc(o1)C(=O)Nc2[nH]c3ccccc3n2	C00995604 (F)	Enamine
21	312	Cc1c2ccccc2oc1C(=O)Nn3cnnc3	C03017636 (F)	Chembridge
22	398	c1ccc2c(c1)cc(o2)C(=O)Nc3ccncc3	C01216648 (F)	Enamine
23	4	c1ccc(cc1)Nc2nccc(n2)c3ccco3	C26643194 (F)	VitasM
24	94	c1ccc(cc1)c2cnc(c(=O)[nH]2)c3ccccc3	C08672863 (F)	Specs

[a]Consensus rank in the screened library. The ZINC fragment (F: 0.8 million compounds) and lead-like (L: 4.6 million compounds) libraries were docked and compounds were selected separately from the two screens.
[b]ZINC code (http://zinc.docking.org/). The screened library is shown in parenthesis.

Table S4. Experimental data for compounds that were active at either the $A_{2A}AR$ or MAO-B. The discovered dual-target ligands are shown in Table 1.

ID	2D structure	$A_{2A}AR$ (K_i/nM or %)[a]	MAO-B (IC_{50}/nM)[b]
6	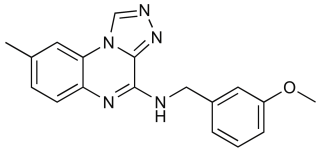	37 ± 1 %	180 ± 10
7	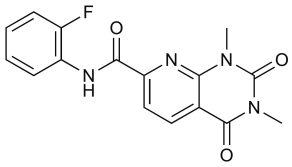	24 ± 4 %	61 ± 17
9	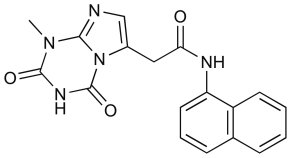	16 ± 4 %	8700 ± 1100
12	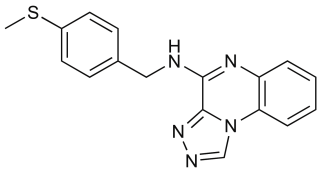	20 ± 4 %	250 ± 24
13	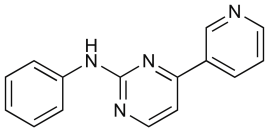	25 ± 3 %	400 ± 36
15	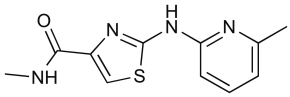	7100 ± 220	53%
18	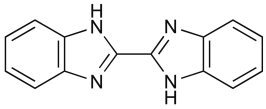	140 ± 69	> 30,000
22	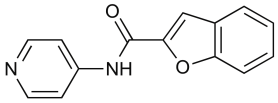	60 ± 2 %	6900 ± 120
23	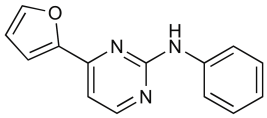	37 ± 4 %	510 ± 47
24	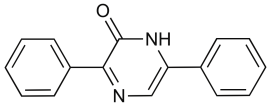	47 ± 3 %	140 ± 10

[a]Percent displacement at 30 μM or K_i value expressed as a mean ± SEM from 2 (%) or 3 (K_i) independent experiments performed in duplicate or triplicate.
[b]Percent inhibition at 30 μM or IC_{50} value expressed as a mean ± SEM from 3 independent experiments performed in duplicate or triplicate.

Table S5. Most similar known $A_{2A}AR$ and MAO-B ligands to the discovered ligands.

ID	2D structure	Closest dual ligand[a]	Closest $A_{2A}AR$ ligands[b]	Closest MAO-B ligands[b]
1	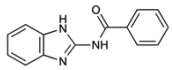	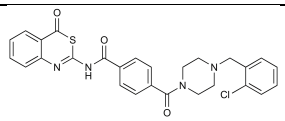	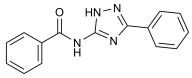	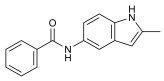
2	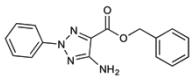	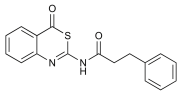	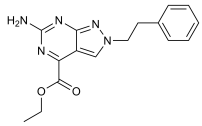	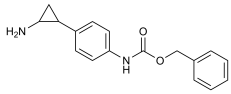
3	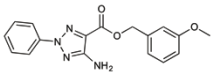	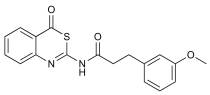	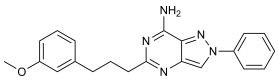	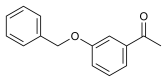
4	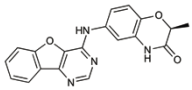	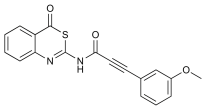	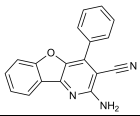	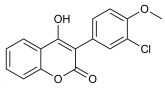

[a]Structure of compound with the maximal Tanimoto coefficient (ECFP4) when compared with all compounds with dual-activity at the $A_{2A}AR$ and MAO-B[3–6] from the ChEMBL database.
[b]Structure of compound with the maximal Tanimoto coefficient (ECFP4) when compared with all known compounds active at the $A_{2A}AR$ or MAO-B, respectively.

Table S6. Smiles and vendor information for analogs of compounds 1 and 3.

ID	Smiles	Vendor
1a	O=C(Nc2nc1cccc(Cl)c1[nH]2)c3ccccc3	Enamine
1b	COc2cccc3[nH]c(NC(=O)c1ccccc1)nc23	Enamine
1c	Cc3ccc2nc(NC(=O)c1ccccc1)[nH]c2c3	Enamine
1d	Cc1cccc(C(=O)Nc2nc3ccccc3[nH]2)c1	VitasM
1e	Cc1ccccc1C(=O)Nc1nc2ccccc2[nH]1	VitasM
1f	Cc1ccc(C(=O)Nc2nc3ccccc3[nH]2)cc1	VitasM
1g	Cc1ccc(C(=O)Nc2nc3ccccc3[nH]2)cc1C	VitasM
1h	COc1cccc(C(=O)Nc2nc3ccccc3[nH]2)c1	VitasM
1i	c1ccc(c(c1)C(=O)Nc2[nH]c3ccccc3n2)O	Enamine
3a	Cc1ccc(COC(=O)c2nn(-c3ccccc3)nc2N)cc1	VitasM
3b	Cc1ccccc1COC(=O)c1nn(-c2ccccc2)nc1N	VitasM
3c	c1ccc(cc1)CNC(=O)c2c(nn(n2)c3ccccc3)N	Enamine
3d	Nc1nc(-c2ccccc2)nn1C(=O)CCc1ccccc1	ChemDiv
3e	Cc1cccc(-c2nc(N)n(C(=O)CCc3ccccc3)n2)c1	ChemDiv
3f	Nc1nc(-c2ccccc2Cl)nn1C(=O)CCc1ccccc1	ChemDiv
3g	Cc1ccc(-c2nc(N)n(C(=O)CCc3ccccc3)n2)cc1	ChemDiv
3h	Cc1ccccc1-c1nc(N)n(C(=O)CCc2ccccc2)n1	ChemDiv
3i	Nc1nc(-c2ccc(Cl)cc2)nn1C(=O)CCc1ccccc1	ChemDiv
3j	Nc1nn(-c2ccccc2)nc1C(=O)O	VitasM
3k	COC1=CC=CC(CO)=C1	SigmaAldrich

Table S7. Experimental data for analogs of compound 1. Analogs with dual-target activity are shown in Table 2.

ID	2D structure	$A_{2A}AR$ (%)[a]
1c	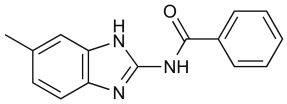	17 ± 1 %
1d	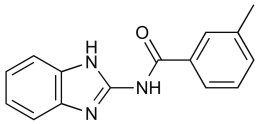	6 ± 3 %
1e	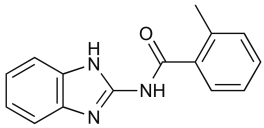	1 ± 1 %
1f	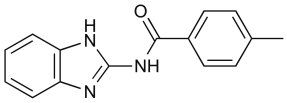	21 ± 4 %
1g	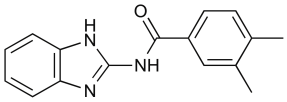	16 ± 4 %
1h	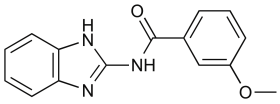	10 ± 4 %
1i	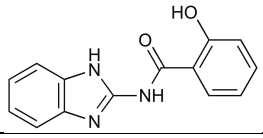	46 ± 5 %

[a]Percent displacement at 10 μM expressed as a mean ± SEM from 2 independent experiments performed in duplicate or triplicate.

Table S8. Experimental data for analogs of compound 3. Analogs that were evaluated at both the $A_{2A}AR$ and MAO-B are shown in Table 2.

ID	2D structure	$A_{2A}AR$ (%)[a]	MAO-B (IC_{50}/nM)[b]
3g	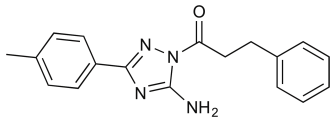	31 ± 3 %	n.d.[c]
3h	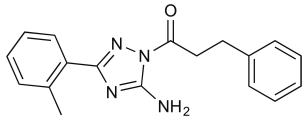	38 ± 1 %	n.d.
3i	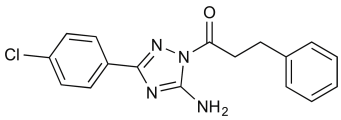	9 ± 3 %	n.d.
3j	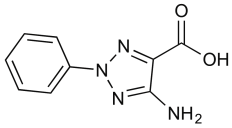	5 ± 4 %	>10000
3k	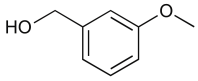	8 ± 2 %	>10000

[a]Percent displacement at 10 μM expressed as a mean ± SEM from 2 independent experiments performed in duplicate or triplicate.
[b]Inactive compounds (>10000 nM) were tested in one experiment performed in triplicate.
[c]Not determined.

Table S9. Summary of available PubChem bioassays (https://pubchem.ncbi.nlm.nih.gov) for compounds 1 and 3.

ID	Inactive[a]	Active[b]	Active (curated)[c]
1	710	39	22
3	766	5	0

[a]Number of PubChem bioassays in which the tested compound was annotated as inactive.
[b]Number of PubChem bioassays in which the tested compound was annotated as active.
[b]Number of PubChem bioassays in which the tested compound was annotated as active and had an activity value < 10 μM or response >50% at this concentration. The identified targets for compound **1** (curated set) are summarized in Table S10.

Table S10. Summary of targets for which compound 1 has significant activity in PubChem bioassays (https://pubchem.ncbi.nlm.nih.gov/).

ID	Target	Activity[a]	BioAssay AID
1	Luciferase[b]	0.2 μM 1.5 μM 88% (10 μM)	773 588342 1006
	ATPase family AAA domain-containing protein 5	0.5 μM	504466
	Ras-related protein Rab-9A	1.6 μM	485297
	Matrix metalloproteinase 1	3.5 μM	618
	Survival of motor neuron 2, centromeric isoform d	4 μM	1458
	RAR-related orphan receptor gamma	6.3 μM 7.9 μM	2551 2546
	Amyloid precursor protein	214% (2 μM)	1276
	Tumor necrosis factor ligand superfamily member 10	62% (5 μM)	1443
	Cytotoxicity to PPC-1 cells	60% (5 μM)	1447
	Heat shock protein 90-alpha	57% (5.9 μM)	1846
	SUMO-1 specific protease 6	95% (10 μM) 91% (12.5 μM)	2599 488915
	SUMO-1/Sentrin specific peptidase 7	93% (5 μM) 100% (12.5 μM)	434973 488917
	SUMO/Sentrin specific protease 8	90% (10 μM) 83% (12.5 μM)	2540 488912
	Caspase-3	96% (12.5 μM)	488918
	Tumor necrosis factor ligand superfamily member 10B	84% (10 μM)	624354
	TWEAK-Fn14 interactions	79% (10 μM)	1159606

[a]Activity value or response at the concentration in parenthesis.
[b]Counterscreen for screening interference with Luciferase-based assays. Compound **1** (based on its similarity to luciferin) is likely to interact with firefly luciferase[7], leading to false positives such assays. The assays performed in this study were not dependent on luciferase.

References

(1) Bento, A. P.; Gaulton, A.; Hersey, A.; Bellis, L. J.; Chambers, J.; Davies, M.; Krüger, F. A.; Light, Y.; Mak, L.; McGlinchey, S.; Nowotka, M.; Papadatos, G.; Santos, R.; Overington, J. P. The ChEMBL Bioactivity Database: An Update. *Nucleic Acids Res.* **2014**, *42*, D1083–D1090.

(2) Mysinger, M. M.; Shoichet, B. K. Rapid Context-Dependent Ligand Desolvation in Molecular Docking. *J. Chem. Inf. Model.* **2010**, *50*, 1561–1573.

(3) Rivara, S.; Piersanti, G.; Bartoccini, F.; Diamantini, G.; Pala, D.; Riccioni, T.; Stasi, M. A.; Cabri, W.; Borsini, F.; Mor, M.; Tarzia, G.; Minetti, P. Synthesis of (E)-8-(3-Chlorostyryl)caffeine Analogues Leading to 9-Deazaxanthine Derivatives as Dual A_{2A} antagonists/MAO-B Inhibitors. *J. Med. Chem.* **2013**, *56*, 1247–1261.

(4) Stößel, A.; Schlenk, M.; Hinz, S.; Küppers, P.; Heer, J.; Gütschow, M.; Müller, C. E. Dual Targeting of Adenosine A_{2A} Receptors and Monoamine Oxidase B by 4 H -3,1-Benzothiazin-4-Ones. *J. Med. Chem.* **2013**, *56*, 4580–4596.

(5) Koch, P.; Akkari, R.; Brunschweiger, A.; Borrmann, T.; Schlenk, M.; Küppers, P.; Köse, M.; Radjainia, H.; Hockemeyer, J.; Drabczyńska, A.; Kieć-Kononowicz, K.; Müller, C. E. 1,3-Dialkyl-Substituted tetrahydropyrimido[1,2-F]purine-2,4-Diones as Multiple Target Drugs for the Potential Treatment of Neurodegenerative Diseases. *Bioorg. Med. Chem.* **2013**, *21*, 7435–7452.

(6) Mikkelsen, G. K.; Langgård, M.; Schrøder, T. J.; Kreilgaard, M.; Jørgensen, E. B.; Brandt, G.; Griffon, Y.; Boffey, R.; Bang-Andersen, B. Synthesis and SAR Studies of Analogues of 4-(3,3-Dimethyl-Butyrylamino)-3,5-Difluoro-N-Thiazol-2-Yl-Benzamide (Lu AA41063) as Adenosine A_{2A} Receptor Ligands with Improved Aqueous Solubility. *Bioorg. Med. Chem. Lett.* **2015**, *25*, 1212–1216.

(7) Thorne, N.; Auld, D. S.; Inglese, J. Apparent Activity in High-Throughput Screening: Origins of Compound-Dependent Assay Interference. *Curr. Opin. Chem. Biol.* **2010**, *14*, 315–324.